Validation of a Single-Cell Reference Model for the Control of a Reconfigurable Battery System

Pinter, Zoltan Mark; Engelhardt, Jan; Rohde, Gunnar; Træholt, Chresten; Marinelli, Mattia

Published in:
Proceedings of 2022 International Conference on Renewable Energies and Smart Technologies

Link to article, DOI:
10.1109/REST54687.2022.10022841

Publication date:
2023

Document Version
Peer reviewed version

Validation of a Single-Cell Reference Model for the Control of a Reconfigurable Battery System

Zoltan Mark Pinter[1], Jan Engelhardt[1], Gunnar Rohde[2], Chresten Træholt[1], and Mattia Marinelli[1]

[1]*Department of Wind and Energy Systems, Technical University of Denmark*, Kongens Lyngby, DK
[2]*Danish Center for Energy Storage*, Copenhagen, DK
{pinzo,janen}@dtu.dk, gr@atv.dk, {ctra,matm}@dtu.dk

***Abstract*—This paper presents the experimental validation of a lithium-iron phosphate cell model. The modelling of dynamic cell behaviour is crucial to improve the performance of reconfigurable battery systems, in which monitoring of the dynamics allows more resoluted leveraging of the battery cells. However, the models of lithium-ion cells are generally inaccurate due to nonlinearities, measurement noise and because the most descriptive state, the state of charge is hidden. Furthermore, the parameter identification of the model requires time and precise measurements, while they differ among the cells, and change as the cells age. The burden of the detailed modelling of a battery system can be alleviated by modelling a single cell, and using the model for each cell in the system. In this work, this possibility is explored by validating a single-cell reference model for a reconfigurable battery system. The terminal voltage residual (error between model and measurement) is presented, and its correlations with internal and external variables are investigated. These correlations can also be used to alleviate the modelling errors. It is concluded that the reference model can qualitatively describe the cell behaviour. By applying small modifications, the model could be used for online estimation.**

***Index Terms*—Model validation, residual analysis, correlation function, battery modelling, battery management systems, state of charge.**

I. Introduction

Decarbonization is a vital topic today, which is partially supported by investment into renewable energy sources and electrical vehicles. In order to compensate for the consequential fluctuation of power in the electrical grid, energy buffers are installed. One of the preferred solutions is using battery energy storage systems (BESS) due to their efficiency and flexibility. These systems consist of a large number of battery cells, and their lifetime and performance is maximized with balanced state of charge (SoC) among the cells [1]. A prominent technique to achieve this is using reconfigurable battery systems, which are capable of engaging or bypassing individual or groups of cells [2].

Modelling the cells is crucial to understand their behaviour [1]. Therefore the investigated lithium-ion cells are interpreted with (Thevenin) equivalent circuit models (ECM), as opposed to the more sophisticated but complicated electrochemical models [3]. Battery packs are generally modelled with a single-cell equivalent, stacking a single model [4], or stacking individual models [5]. Although [6], [7] show that the single-cell equivalents are more accurate than the stacked versions, reconfiguration requires knowledge about individual cells.

The SoC is an interpretation of charge level, and it is a latent (non-measurable) variable. Knowing its value, and its exact mapping to the other physical variables would reduce the burden on planning battery operation. Two rudimentary methods of estimating the SoC are integrating the cell current (coulomb counting) or backtracking it from the open circuit voltage (OCV) [1]. The former introduces bias and ignores phenomena like rate capacity effect [8], while the latter is subject to high level of uncertainty (for LiFePO4/LFP cells) in the middle of the SoC range due to the low voltage measurement accuracy and the inaccuracy of the parameters.

Another benefit of cell modelling and SoC estimation is the improved estimate of the terminal voltage of each cell without measurement noise, from the OCV and the ECM parameters. An example application is voltage and impedance matching for EV charging from a stationary battery system [9]. Due to the nature of cell switching, it is challenged by the current transients [10]. Apart from introducing power converters (which decrease efficiency) or applying pulse width modulation (PWM) on the cell switches [11], selecting cells with well-known OCV and impedance can alleviate the challenge.

The adequacy of a model can be investigated with model validation. For this, the residual (or residual signal) $\tilde{x}$ is defined as the difference of the model output $\hat{x}$ and the measured value x, i. e.

$$\tilde{x} = \hat{x} - x. \tag{1}$$

The basis of model validation is generally investigating the autocorrelation function (ACF) and the cross-correlation functions (CCF) with the inputs [12]. For nonlinear systems like ours, further higher order cross-correlations may be explored [13], [14].

Contribution

Cell modelling requires time and precise experimental setups, and the found parameters depend on several variables like current, temperature or aging [1]. In order to save time and energy in this process, the model of one single cell could be used to describe the behaviour of each cell in a battery system.

This work has received funding from the IFD funded TOPchargE project under the Grant Agreement No. 9090-00035A (http://topcharge.eu/)

978-1-6654-0971-1/22/$31.00 ©2022 IEEE

The contribution of this work is the model validation of this reference model, based on the terminal voltage residual. The model accuracy and the dynamic response is used to find the applicability of this reference model, which can be

- prediction of the model states, if the residual has low autocorrelation and its mean is bounded by 5 mV,
- estimation of the model states, if the residual mean is bounded by 20 mV, and the estimator is faster than the system dynamics,
- qualitative investigation of a controller, using the model as a testing environment, if the residual mean is bounded by 50 mV.

One outcome of the model validation is the decision about this applicability. Moreover, it is found if the reference model can be used as it is, it needs to be modelled again with new considerations, or it needs augmentation with online or offline estimation for each cell.

The paper is structured as follows. Section II-A describes the BESS used for the model validation. Section II-B presents the modelling done for the single cell reference model. Section III describes the methodology and Section IV the results of the model validation. Section V discusses the results and Section VI concludes the paper.

II. Investigated Battery System

A. System description

The investigated BESS is a reconfigurable battery string designed as a stationary buffer for EV charging, with the cells connected in series. As the BESS is connected to the AC grid via a power converter, which has maximum efficiency at 800 V, this value is kept by the BESS. The string consists of 11 modules, and one battery module has 27 cells [15]. Since the results found for individual modules align well, one single module is depicted here. Assuming that the accuracy deterioration due to the voltage divider is negligible, the cell voltage measurement accuracy of the PIC microcontroller is 0.08 % of the nominal cell voltage of 3.2 V, which is $\approx 3\,\mathrm{mV}$. The Murata temperature sensor has the self-heating of 1°C, and its time constant is below 2 minutes. The deployed SET transducer measures the string current with 1% accuracy, which is maximum $0.43\,\mathrm{A}$ for the tests following. The measurements are logged every 0.5 seconds.

B. Cell model description

The LFP cells used in the experimental setup have a nominal capacity of 100 Ah [15], and this value is considered for all of the cells. One reference cell was characterized and modelled with a second order Thévenin equivalent (see Fig. 2b), which finds the terminal voltage in the Laplace domain as

$$\hat{V} = \hat{V}_{OC} - I\left(\hat{R}_0 + \frac{\hat{R}_1}{\hat{\tau}_1 \mathrm{s} + 1} + \frac{\hat{R}_2}{\hat{\tau}_2 \mathrm{s} + 1}\right), \qquad (2)$$

where I is the cell current, the ECM parameters are the resistances R_i and capacitances C_i, giving the time constants $\tau_i = R_i C_i$. Note that this assumes a locally linear model.

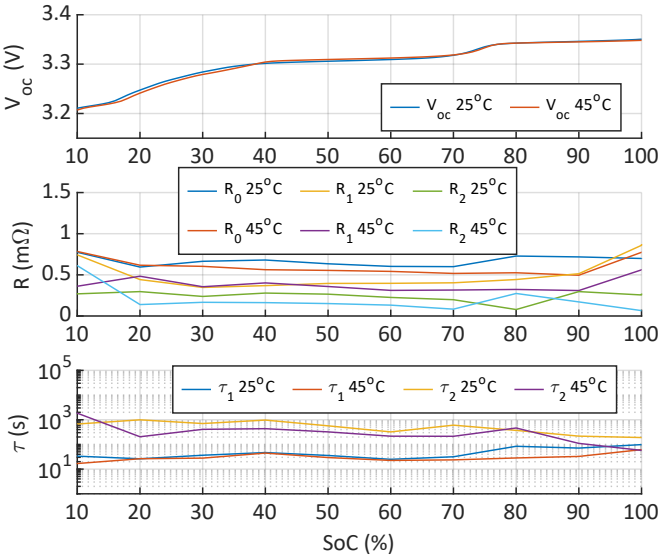

Fig. 1. Open-circuit voltage (OCV), resistances and time constants as a function of cell state-of-charge (SoC) for the reference cell model

The progression of the open-circuit voltage (OCV or V_{OC}) was determined by measuring the voltage at currents of 3.5 A (discharging) and -3.5 A (charging), and averaging the two curves. As seen in Fig. 1, the OCV has a relatively constant trend including a plateau with nearly zero gradient around 50 % SoC. Furthermore, pulse charging experiments were conducted to estimate the values of the ECM parameters at different SoC. The current was controlled to form pulses of 100 A (1C) for 6 minutes followed by a relaxation time of 90 minutes [16]. Note that due to the nature of the tests, the OCV and the ECM parameter estimates are interdependent and hence introduce error. To consider the influence of cell temperature, all experiments were performed in a climate chamber at $25\,^{\circ}\mathrm{C}$ and $45\,^{\circ}\mathrm{C}$ and the estimated parameters were modelled with linear interpolation in between. It is assumed that the hysteresis [1] is negligible and the ECM parameters have no current dependency. To avoid adding further nonlinearities to the model, the ECM parameters were averaged for the values from the charging and discharging experiments. For the experiments and the model validation, the SoC was estimated with coulomb counting, i. e. $\Delta SoC = \int I dt$, and it was reset to 0% and 100% at 2.8 V and 3.4 V (as here better accuracy is expected).

III. Methodology

In order to explore individual aspects of the model, different scenarios were designed. A full charge and a full discharge were made at a typical EV charging power level of $\pm 25\,\mathrm{kW}$. Apart from the limitations due to the voltage granularity, the constant power leads to nearly constant current, ranging between 31.5 A and 32.0 A. Fig. 3 and Fig. 4 (bottom) present the cell voltage measurement for such a test. Ideally, this is an even swipe through the average SoC range of the whole BESS. The average SoC is denoted by $\overline{\mathrm{SoC}}$ from now on, and

it is understood for the whole battery system. Apart from the mentioned tests, there were 12 Parker tests made [17]. These tests are to find the quality of setpoint following of a system. Hereby it is used to trigger the dynamic response to steps, ramps and harmonic signal, without having a notable effect on the SoC. The 12 tests are made at 4 different $\overline{\text{SoC}}$ values with 3 frequencies of power requests. Fig. 4 (top) depicts the corresponding current, which is shared by all the engaged cells, at 65% $\overline{\text{SoC}}$. Before each scenario, the cells were entirely charged or discharged to minimize the bias.

The inputs to the model are the current and the temperature. Both the reference model and the model validation tests used temperature measured at the top of the battery cell. This temperature is different from the average temperature of the cell. These measurements range between 25 and 32 degrees for all data, and range maximum 3 degrees for individual cells. Moreover, they do not correlate with the residuals. Therefore it is assumed that the effect of temperature on the residuals cannot be quantified.

Fig. 2a depicts that the inputs to the cell model are the (binary) engagement signal Γ_i (value 0 referring to bypassing, and 1 to engagement), the string current I_{string} and the temperature. The cell current is $I = \Gamma_i I_{\text{string}}$. The output is the terminal voltage $\hat{V}_i$. The residual is then compared against different variables to focus on different aspects of the modelling errors. The summary of statistics for the test scenarios are then compared in Table I.

IV. Results

Fig. 3 shows how large the variance of the voltage measurements is, hence it is impractical to deduce the SoC at the plateau between 30 and 120 minutes. Due to the differences in capacities, cells reach the minimum limit of 2.8 V earlier at different times. Since the model assumes a cell capacity of 100 Ah, this means that the SoC estimate will always introduce errors to the OCV and ECM parameters.

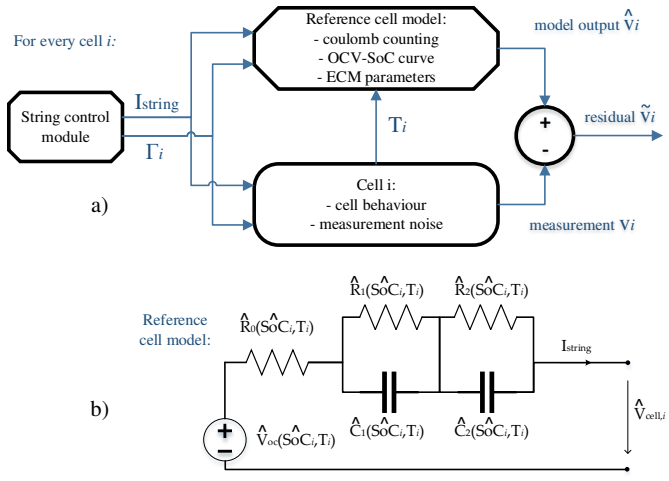

Fig. 2. *a)* The methodology of extracting the residual. Note that the model is the same for each cell. *b)* The Thévenin equivalent with the ECM parameters

The 27 residuals for the full discharge are plotted against the SoC after taking the moving average for 100 sample points in Fig. 5. The statistics in Table I refer to this interpretation, where the union of the cells is taken to deduce the mean $\mu_\cup$ and the standard deviation $\sigma_\cup$. Furthermore, the mean value μ_i was calculated for each cell i, then the median M_μ, the interquantile range IQR_μ, the range R_μ, and the average of the individual standard deviations $\overline{\sigma}$ is presented. Regarding the histogram in Fig. 5, it can be seen that the residuals do not follow a Gaussian distribution. They are more Gaussian for the Parker tests, since those are around the OCV-SoC plateau. The envelopes of the residuals for charging and discharging are also depicted. Generally, the model performs poorly below 30% $\overline{\text{SoC}}$, since in this region, the parameters of the reference model are not representative for the BESS and are asymmetric for charging and discharging. As a result of the heterogeneity of the capacities and the consequential bias in the coulomb counting, there are negative spikes at 95% $\overline{\text{SoC}}$ for charging.

The string current for the two tests is $\approx \pm 31.75$ A, however, the Parker tests range between $\approx \pm 43$ A. Therefore we expect to see larger errors for the latter. Assuming that the current, the temperature, the ECM parameter asymmetry and the hysteresis are negligible, and the cell SoC is not effected by the short durations of current, the residual only depends on the current as variable. Since I does not spread evenly along its range due to the nature of switching, plotting the residuals against the cell voltage is more informative. Fig. 6 depicts a heat map for the union of cells. Since the Parker test input has zero mean, the peak is around the average OCV value, hence the cells are most likely to rest at this value. The average OCV is ≈ 3.31 V, overestimated by 20 mV. Experiments show that subtracting this value from the OCV-SoC lookup table vanishes $\mu_\cup$.

If the assumptions hold, it can be shown that the slope m at any time can be described by $m = \Delta\tilde{V}/\Delta\hat{V}$. In case of steady state, $m = 1 - \frac{\hat{R}_0+\hat{R}_1+\hat{R}_2}{\hat{R}_0+\hat{R}_1+\hat{R}_2}$ is the slope of the fitted line for a cell, and it could be used to adjust the resistance to the correct value (the idea is taken from Lissajous curves [18]). However, when the differential of the residual is investigated, it can be seen that the steps (jumps) of the Parker test (see Fig. 4) dominate the spread of the points. Hence the resistance error is negligible compared to either the time constant errors or the error due to the hysteresis. Fig. 7 shows that the residual and

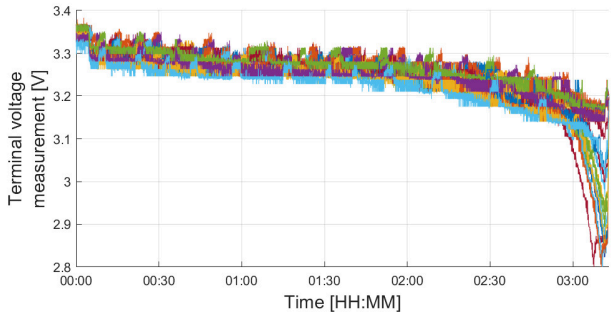

Fig. 3. Measured voltage of 27 cells, full discharge with ≈ 32 A string current

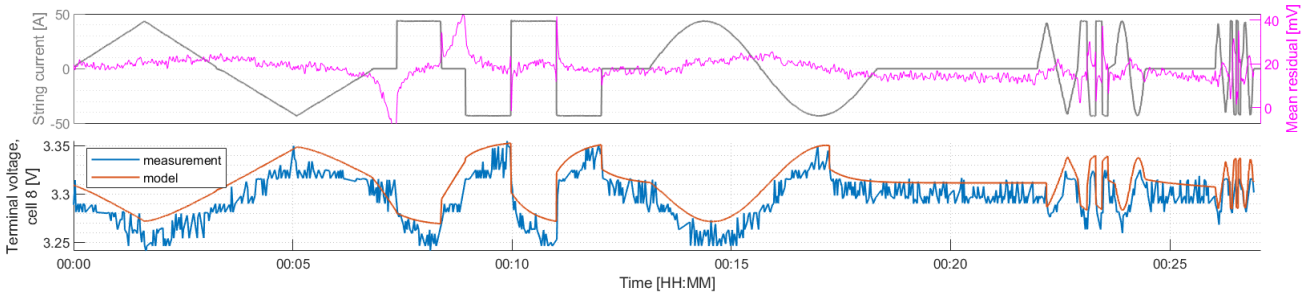

Fig. 4. Parker test [17], 65% $\overline{\text{SoC}}$, top: the corresponding residual averaged for the cells, bottom: the terminal voltage for the model and measurement

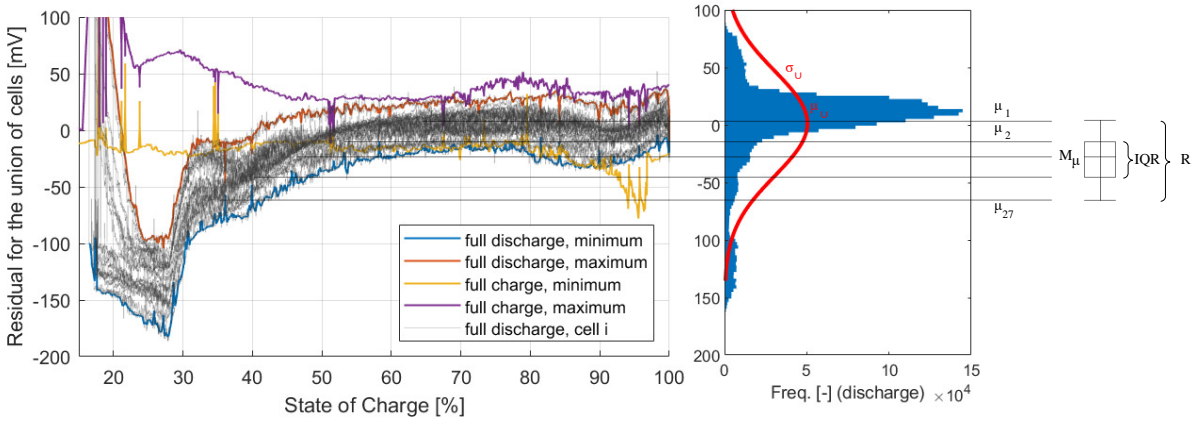

Fig. 5. Residuals envelopes against SoC; for the discharge test: individual residuals and the statistics (histogram and boxplot) used in Table I

current input ACF peaks coincide, e. g. at 12.5 minutes. This is the time between the ramp and the sinusoidal. Therefore the ACF cannot be used for qualifying the model validation.

Table I compares the statistics of the 6 test scenarios. The union mean $\mu_\cup$ ranges between -21 and 42 mV. Its asymmetry for charge and discharge indicates asymmetry of the parameters. It is larger for the Parker tests due to the larger currents. It increases away from the OCV-SoC plateau because of the OCV-SoC curvature at these points. The union standard deviation $\sigma_\cup$ is notably lower for the Parker tests at larger $\overline{\text{SoC}}$, which indicates that the lookup parameters are more uniform for the cells at this region. The median M_μ changes sign around the OCV-SoC plateau, due to the individuality of the reference model. For the same reason, IQR_μ and R_μ have the 35% $\overline{\text{SoC}}$ Parker test results outstandingly wrong. Regarding $\overline{\sigma}$, the precision is bounded by 10 mV for most of the $\overline{\text{SoC}}$ range and a bit larger for the full charge and discharge tests, since these explore the edges of the OCV-SoC curve.

Test	$\mu_\cup$	$\sigma_\cup$	M_μ	IQR_μ	R_μ	$\overline{\sigma}$
full charge	14	31	19	29	55	18
full discharge	-21	46	-21	26	56	20
Parker test, 30% $\overline{\text{SoC}}$	43	43	-47	15	223	11
Parker test, 35% $\overline{\text{SoC}}$	30	27	-36	33	99	10
Parker test, 65% $\overline{\text{SoC}}$	18	12	18	12	41	7
Parker test, 80% $\overline{\text{SoC}}$	42	13	41	12	44	8

TABLE I
STATISTICS OF THE 6 SCENARIOS. ALL ARE UNDERSTOOD IN [MV]

V. DISCUSSION

From the plots, the quality of the OCV-SoC curve can be found and improved. The effect of the missing time constants or the hysteresis on the residual cannot be quantified, as the residual and residual and the current input signals correlate, having peaks at the same locations. Ideally white noise with adequate bandwidth could be imposed as current input, without bypassing cells, to find the ACF and CCF. Alternatively PRBS input signal [19] could be used, alleviating the requirements on the actuator. Currently these inputs are not possible with the investigated BESS. If the nonlinearities are negligible, and the SoC is constant, tools of correlation could quantify the effect of the missing dynamics. Then the parameters could be tailored to decrease the ACF values.

The strategy of using one single cell to determine the reference model is time and energy efficient, but simplistic, given the values of IQR_μ and R_μ. Alternatively a group of cells could be selected randomly from the BESS. Fig. 5 shows that 27 cells create a smooth distribution. Furthermore, the online estimation of the individual capacities could significantly reduce the bias from coulomb counting.

More sophisticated tests would improve the interdependence of the identification of the OCV-SoC and ECM parameters. However, this is impractical due to the necessary time, when further decreasing the current or introducing resting times.

The residual mean is bounded by 50 mV. Therefore regarding the applicability of the reference model, it can be used for

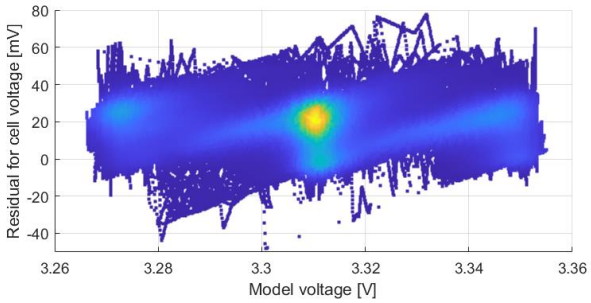

Fig. 6. Residual heat map against model voltage for a Parker test, 65% $\overline{\text{SoC}}$

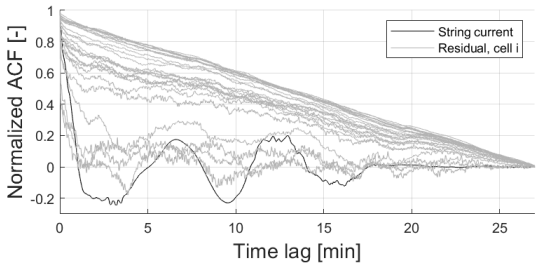

Fig. 7. ACF for a Parker test at 65% $\overline{\text{SoC}}$, for every cell and the string current

a qualitative analysis of a controller, by adequately changing model parameters to emulate the heterogeneity of the cells. In case it is augmented with an online data driven method for each cell, it is possible to use it for online estimation. For example, the individual cell residuals could be whitened from correlations with an ARMAX model [20], and the found filters could be added to the reference model as a dual estimator of states and parameters. Alternatively, nonlinear estimators could be applied from the field of machine learning. However, using a data driven approach is for the cost of losing some understanding of the model.

VI. Conclusion

In this work, model validation was used to find the applicability of a single cell reference model. This model was used to estimate the behaviour of each cell in a reconfigurable battery system. First, the modelling strategy for the reference (Thévenin equivalent circuit) model was presented. Then the test scenarios were described, which were designed to investigate individual aspects of the model. The residuals were defined as the error between the model and the measurements, for the terminal voltage. Their dependencies on the average SoC range, the internal and the external variables were investigated. Using the findings, the model bias could be alleviated. Finally, the statistics of the different scenarios were discussed.

To summarize, the single cell reference model is an adequate model to test a controller. Model augmentation could help to improve its accuracy and to use it as an online estimator, for example with online linear parameter estimation, or with a nonlinear estimator.

Acknowledgment

The authors are grateful to Andreas Thestrup Valgreen and Søren Schmidt Petræus for their contribution to the battery modelling. We also thank to Gergő Kiss for his technical support with using the battery management system.

References

[1] G. L. Plett, *Battery management systems, Volume I: Battery modeling*. Artech House, 2015.

[2] Z. M. Pinter, D. Papageorgiou, G. Rohde, M. Marinelli, and C. Træholt, "Review of control algorithms for reconfigurable battery systems with an industrial example," in *2021 56th International Universities Power Engineering Conference (UPEC)*. IEEE, 2021, pp. 1–6.

[3] L. D. Couto and M. Kinnaert, "Partition-based unscented kalman filter for reconfigurable battery pack state estimation using an electrochemical model," in *2018 Annual American Control Conference (ACC)*. IEEE, 2018, pp. 3122–3128.

[4] C. Parthasarathy, H. Hafezi, and H. Laaksonen, "Lithium-ion bess integration for smart grid applications-ecm modelling approach," in *2020 IEEE Power & Energy Society Innovative Smart Grid Technologies Conference (ISGT)*. IEEE, 2020, pp. 1–5.

[5] A. Mondoha, J. Sabatier, P. Lanusse, S. Tippmann, and C. Farges, "Nonlinear model predictive control for a simulated reconfigurable battery pack," *IFAC-PapersOnLine*, vol. 54, no. 6, pp. 353–358, 2021.

[6] A. S. Subburaj and S. B. Bayne, "Analysis of dual polarization battery model for grid applications," in *2014 IEEE 36th International Telecommunications Energy Conference (INTELEC)*. IEEE, 2014, pp. 1–7.

[7] O. M. Akeyo, V. Rallabandi, N. Jewell, A. Patrick, and D. M. Ionel, "Parameter identification for cells, modules, racks, and battery for utility-scale energy storage systems," *IEEE Access*, vol. 8, 2020.

[8] N. Lin, S. Ci, D. Wu, and H. Guo, "An optimization framework for dynamically reconfigurable battery systems," *IEEE Transactions on Energy Conversion*, vol. 33, no. 4, pp. 1669–1676, 2018.

[9] J. Engelhardt, J. M. Zepter, T. Gabderakhmanova, G. Rohde, and M. Marinelli, "Double-string battery system with reconfigurable cell topology operated as a fast charging station for electric vehicles," *Energies*, vol. 14, no. 9, p. 2414, 2021.

[10] J. Engelhardt, T. Gabderakhmanova, G. Rohde, and M. Marinelli, "Reconfigurable stationary battery with adaptive cell switching for electric vehicle fast-charging," in *2020 55th International Universities Power Engineering Conference (UPEC)*. IEEE, 2020, pp. 1–6.

[11] E. Chatzinikolaou and D. J. Rogers, "Hierarchical distributed balancing control for large-scale reconfigurable ac battery packs," *IEEE Transactions on Power Electronics*, vol. 33, no. 7, pp. 5592–5602, 2017.

[12] V. M. Marques, C. J. Munaro, and S. L. Shah, "Detection of causal relationships based on residual analysis," *IEEE Transactions on Automation Science and Engineering*, vol. 12, no. 4, pp. 1525–1534, 2015.

[13] L. Fortuna, S. Graziani, A. Rizzo, M. G. Xibilia *et al.*, *Soft sensors for monitoring and control of industrial processes*. Springer, 2007, vol. 22.

[14] S. Billings and Q. Zhu, "Nonlinear model validation using correlation tests," *International journal of control*, vol. 60, no. 6, 1994.

[15] "Sinopoly battery, "model: Sp-lfp100aha," datasheet," http://www.sinopolybattery.com/userfiles/files/SP-LFP100AHA.pdf. Accessed: Oct. 25, 2021.

[16] S. e. a. Valgreen, "Performance characterisation and dynamical behaviour of a reconfigurable battery system," *Master thesis*, 2021.

[17] A. Zecchino, A. Thingvad, P. B. Andersen, and M. Marinelli, "Test and modelling of commercial v2g chademo chargers to assess the suitability for grid services," *World Electric Vehicle Journal*, vol. 10, no. 2, 2019.

[18] K. Palmer, T. Ridgway, O. Al-Rawi, I. Johnson, and M. Poullis, "Lissajous figures: an engineering tool for root cause analysis of individual cases—a preliminary concept," *The Journal of extra-corporeal technology*, vol. 43, no. 3, p. 153, 2011.

[19] E. Namor, F. Sossan, E. Scolari, R. Cherkaoui, and M. Paolone, "Experimental assessment of the prediction performance of dynamic equivalent circuit models of grid-connected battery energy storage systems," in *2018 IEEE PES Innovative Smart Grid Technologies Conference Europe (ISGT-Europe)*. IEEE, 2018, pp. 1–6.

[20] H.-T. Yang, C.-M. Huang, and C.-L. Huang, "Identification of armax model for short term load forecasting: an evolutionary programming approach," in *Proceedings of Power Industry Computer Applications Conference*. IEEE, 1995, pp. 325–330.